

Spin-dependent heat signatures of single-molecule spin dynamics

H. Hammar, J. D. Vasquez Jaramillo, and J. Fransson

Department of Physics and Astronomy, Uppsala University, Box 530, SE-751 21 Uppsala

(Dated: June 29, 2022)

We investigate transient spin-dependent thermoelectric signatures in a single-molecule magnet under the effect of a time-dependent voltage pulse. We model the system using non-equilibrium Green's functions and a generalized spin equation of motion incorporating the dynamic electronic structure of the molecule. We show that the generated heat current in the system is due to both charge and spin contributions, related to the Peltier and the spin Peltier effect. There is also a clear signature in the heat current due to the spin-driven heat flow and a possibility to control the spin-dependent heat currents by bias, tunneling coupling and pulses. A reversal of the net heat transfer in the molecule is found for increasing bias voltage due to the spin-dependent heat transfer and we can correlate the net heat transfer with the anisotropies in the system.

I. INTRODUCTION

Thermoelectricity and thermodynamics in nanosystems, such as single-molecules and nanojunctions, have been under investigation during recent years [1]. Together with the experimental realizations and control of single-molecule magnets (SMMs), and the extension of conventional thermoelectrics to include spin degrees of freedom, this has led to the conjunction of spin-dependent thermoelectric effects in nanoscale systems.

Spin-dependent thermoelectricity has been studied in several different molecular systems and quantum dots [7–9, 12–22]. Furthermore, other studies involve the effect of time-dependent control on the energy and heat transfer of molecular systems [23–27] to, e.g., improve the thermoelectric efficiency or design thermal machines. Similarly, electrical and thermal control of, e.g., local interactions and anisotropies in SMMs have been demonstrated both experimentally and theoretically [28–39], thus, defining new realms for engineered driven nanoscale thermoelectric devices containing SMMs.

The discovery of the spin Seebeck and spin Peltier effect led to further increase the interest in spin-dependent thermoelectric effects [2–6]. It also includes investigations of the spin-dependent Seebeck and Peltier effect where the heat current is coupled to the spin-dependent electron channels in the material. In the context of SMMs, local anisotropies have been suggested to have an effect on the spin-dependent thermoelectric transport properties [7–9]. Experiments of SMMs show thermodynamic signatures of the change of spin configurations in the magnet [10], similar to the effect of spin entropy in bulk materials [11].

Strongly coupled nanoscale devices also introduces new challenges for how we perceive and understand nature, specially at the nanoscale. Quantum thermodynamics has been under recent investigation, where in the case of driven systems the classical framework has been extended to include system-bath coupling and time-dependent drives [40–43]. In order to comply with the laws of thermodynamics, the local nanoscale system has to include the coupling to the environment, as well as internal entropy production [44, 45]. Recent results show much progress in finding consistent laws, although, not much has been done in the context of magnetic systems and SMMs.

In this paper, we investigate spin-dependent effects in the

heat current in a SMM and the effect of the spin dynamics in the heat flow. We model the system as a local magnetic moment coupled to a quantum dot (QD) between two magnetic leads where we apply a pulse across the junction, see Fig. 1. We show that the generated heat current in the junction can both be related to the transport of charges, i.e., related to the conventional thermoelectric effects, and by the spin transport in the system, i.e., related to spin-dependent thermoelectric effects. This can in turn be related to the spin-dependent and spin Peltier effect and we show clear signatures of spin-dependent heat flow in the system.

Our results show a reversal of the net heat transfer for an increased bias voltage due to the spin-dependent net heat transfer in the system. For increasing tunneling couplings the system will be more damped and the uniaxial anisotropies of the SMM diminish as well as the spin contribution in the net heat transfer. By applying a pulse, we can create transient heat currents that both can serve as a probe of the spin switching in the system as well as to increase the thermoelectric efficiency of SMM devices.

The paper is organized as follows. In Sec. II we lay out the theoretical background to the study. This includes general background to thermoelectricity in a SMM, the specific model

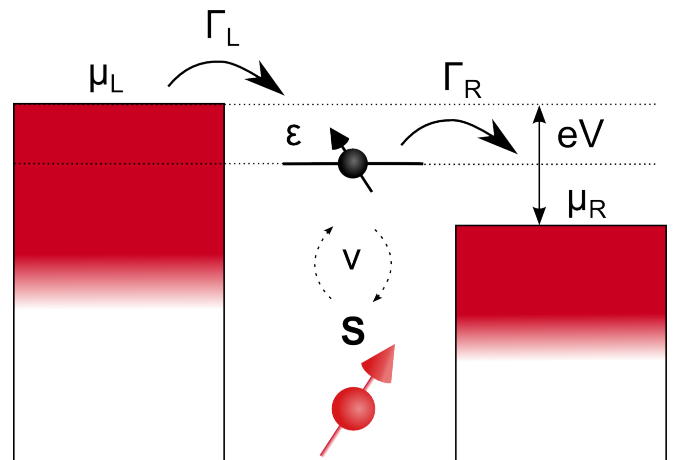


FIG. 1: The system studied in this work, consisting of a local magnetic moment coupled to a quantum dot in a tunnel junction between magnetic leads.

under study, heat current with charge- and spin-dependent parts and a brief review of the single-molecule spin dynamics employed in the study. In Sec. III we show the results of our numerical simulations and in Sec. IV we conclude the paper.

II. THEORY

A. Thermoelectricity in a single-molecule magnet

The thermoelectric effects of a single-molecule magnet can be related by the Onsager matrix in linear response [8, 9]. Thus, by a voltage, spin, or thermal bias, currents of both charge, spin, and heat character can be driven through the system. In linear response one can define the Seebeck coefficient, Peltier coefficient, and their spin-dependent counterparts. As we are not treating linear response in this paper we will not define these quantities, although, the effects that they describe serve as a good ground for the physics that we want to describe.

There are two different types of spin related thermoelectrical effects in literature. One is considered as spin-dependent Seebeck and spin-dependent Peltier effect, where the spin transfer is driven by the transport of charges in the junction. The second is known as spin Seebeck and spin Peltier effect, where the effect is a collective phenomena that requires no charge transfer, i.e. $I_C = 0$. In both cases the resulting effect is that a thermal bias creates a spin bias (Seebeck) and that a spin bias creates a thermal bias in the system (Peltier) which results in a spin and heat current, respectively.

In the case of a SMM that exhibits a local magnetic moment, as is considered in this article, both effects will take place. Partly there is spin-dependent Seebeck and Peltier effect due to the net transport of spins related to the charges in the system. A finite spin Seebeck and spin Peltier do also exist and a single-molecule magnet can exhibit pure spin currents [7–9, 16]. The case is also true for a quantum dot under a magnetic field or connected to ferromagnetic leads [13, 46]. As the system under study has these properties the total spin-driven heat current will thus be both due to the spin Peltier effect as well as the spin-dependent Peltier effect.

B. Model system

We consider a magnetic molecule, embedded in a tunnel junction between metallic leads, comprising a localized magnetic moment \mathbf{S} coupled via exchange to the highest occupied or lowest unoccupied molecular orbital henceforth referred to as the QD level. The system is shown in Fig. 1 and we define our system Hamiltonian as

$$\mathcal{H} = \mathcal{H}_L + \mathcal{H}_R + \mathcal{H}_T + \mathcal{H}_{QD} + \mathcal{H}_S. \quad (1)$$

Here, $\mathcal{H}_\chi = \sum_{\mathbf{k}\sigma\epsilon_\chi} (\epsilon_{\mathbf{k}\chi} - \mu_\chi) c_{\mathbf{k}\chi\sigma}^\dagger c_{\mathbf{k}\chi\sigma}$, is the Hamiltonian for the left ($\chi = L$) or right ($\chi = R$) lead, where $c_{\mathbf{k}\chi\sigma}^\dagger$ ($c_{\mathbf{k}\chi\sigma}$) creates (annihilates) an electron in the lead χ with energy $\epsilon_{\mathbf{k}\chi}$,

momentum \mathbf{k} , and spin $\sigma = \uparrow, \downarrow$, while μ_χ denotes the chemical potential such that the voltage V across the junction is defined by $eV = \mu_L - \mu_R$. Tunneling between the leads and the QD level is described by $\mathcal{H}_T = \mathcal{H}_{TL} + \mathcal{H}_{TR}$, where $\mathcal{H}_{T\chi} = T_\chi \sum_{\mathbf{k}\sigma\epsilon_\chi} c_{\mathbf{k}\chi\sigma}^\dagger d_\sigma + H.c..$ The single-level QD is represented by $\mathcal{H}_{QD} = \sum_\sigma \epsilon_\sigma d_\sigma^\dagger d_\sigma$, where d_σ^\dagger (d_σ) creates (annihilates) an electron in the QD with energy $\epsilon_\sigma = \epsilon_0 + g\mu_B B^{\text{ext}} \sigma_z / 2$ and spin σ , depending on the external magnetic field $\mathbf{B}^{\text{ext}} = B^{\text{ext}} \hat{\mathbf{z}}$, where g is the gyromagnetic ratio and μ_B the Bohr magneton. The energy of the local spin is described by $\mathcal{H}_S = -g\mu_B \mathbf{S} \cdot \mathbf{B}^{\text{ext}} - v\mathbf{s} \cdot \mathbf{S}$ where v is the exchange integral between the localized and delocalized electrons, the electron spin is denoted $\mathbf{s} = \psi^\dagger \boldsymbol{\sigma} \psi / 2$ in terms of the spinor $\psi = (d_\uparrow \ d_\downarrow)$, and $\boldsymbol{\sigma}$ is the vector of Pauli matrices.

The dynamical QD electronic structure is calculated by using nonequilibrium Green's functions (GF), defined on the Keldysh contour $\mathbf{G}(t, t') = \theta(t - t') \mathbf{G}^>(t, t') + \theta(t' - t) \mathbf{G}^<(t, t')$. We take into account the back action from the local spin dynamics by perturbation theory, expanding to first order in the time-dependent expectation value of the spin according to

$$\mathbf{G}(t, t') = \mathbf{g}(t, t') - v \oint_C \mathbf{g}(t, \tau) \langle \mathbf{S}(\tau) \rangle \cdot \boldsymbol{\sigma} \mathbf{g}(\tau, t') d\tau. \quad (2)$$

Here, $\mathbf{g}(t, t')$ is the bare QD GF defined as a 2×2 -matrix in spin space. It is defined by the equation

$$(i\partial_t - \epsilon) \mathbf{g}(t, t') = \delta(t - t') \sigma^0 + \int \Sigma(t, \tau) \mathbf{g}(\tau, t') d\tau, \quad (3)$$

where ϵ is the matrix of spin-dependent energy levels of the QD and the self-energy is defined as $\Sigma(t, t') = \sum_\chi \sum_{\mathbf{k}\epsilon_\chi} |T_\chi|^2 \mathbf{g}_{\mathbf{k}\sigma}(t, t')$, where $\mathbf{g}_{\mathbf{k}\sigma}(t, t')$ is the GF for electrons in the lead.

Solving for the magnetic lead GF, the self-energies can be expressed as

$$\Sigma^{</>}(t, t') = (\pm i) \sum_\chi \Gamma^\chi \int f_\chi(\pm\omega) e^{-i\omega(t-t') + i \int_t^{t'} \mu_\chi(\tau) d\tau} \frac{d\omega}{2\pi}, \quad (4)$$

where we introduced the coupling matrix $\Gamma^\chi = \Gamma_0^\chi \sigma^0 + \Gamma_1^\chi \cdot \boldsymbol{\sigma}$ and defined the tunneling coupling $\Gamma_\sigma^\chi = 2|T_\chi|^2 \sum_{\mathbf{k}\epsilon_\chi} \delta(\omega - \epsilon_{\mathbf{k}\sigma})$, $\Gamma_0^\chi = \sum_\sigma \Gamma_\sigma^\chi$ and $\Gamma_1^\chi = \sum_\sigma \sigma_\sigma^\chi \Gamma_\sigma^\chi \hat{\mathbf{z}}$ using the wide-band limit. By introducing the spin-polarization in the leads $p_\chi \in [-1, 1]$, such that $\Gamma_\sigma^\chi = \Gamma_0^\chi (1 + \sigma_\sigma^\chi p_\chi) / 2$, we can write $\Gamma_1^\chi = p_\chi \Gamma_0^\chi \hat{\mathbf{z}}$. Using similar notation we can write the lesser/greater Green's function and self-energies as $\mathbf{G} = \mathbf{G}_0 \sigma^0 + \boldsymbol{\sigma} \cdot \mathbf{G}_1$ and $\Sigma^{</>} = \Sigma_0^{</>} \sigma^0 + \Sigma_1^{</>} \cdot \boldsymbol{\sigma}$. We refer to Ref. [36] for more details.

The self-energy carries the information of an on-set of voltage in the system or that of a pulse due to the time integration of the chemical potential for each lead, i.e., $i \int_t^{t'} \mu_\chi(\tau) d\tau$. Thus, this initiates the dynamics in the system and carries the information of the pulse.

C. Heat and energy currents

The properties of the QD are probed by means of the heat and energy currents flowing through the system. In this way, the goal is to pick up signatures of the spin dynamics in the thermoelectric transport properties. We start by defining the particle, energy and heat current, I^N , I^E and I^Q , respectively. Accordingly, we define

$$I_\chi^N(t) = -\partial_t \sum_{\mathbf{k}\sigma \in \chi} \langle n_{\mathbf{k}\sigma} \rangle = \frac{i}{\hbar} \sum_{\mathbf{k}\sigma} \langle [c_{\mathbf{k}\sigma\chi}^\dagger c_{\mathbf{k}\sigma\chi}, \mathcal{H}] \rangle, \quad (5a)$$

$$I_\chi^E(t) = -\partial_t \sum_{\mathbf{k}\sigma \in \chi} \langle \mathcal{H}_\chi \rangle = \frac{i}{\hbar} \sum_{\mathbf{k}\sigma} \varepsilon_{\mathbf{k}\sigma} \langle [c_{\mathbf{k}\sigma\chi}^\dagger c_{\mathbf{k}\sigma\chi}, \mathcal{H}] \rangle, \quad (5b)$$

$$I_\chi^Q = I_\chi^E - \mu_\chi I_\chi^N. \quad (5c)$$

Here, we ignore the energy reactance from the tunneling Hamiltonian in the energy current as suggested in Ref. [40, 42]. This as we have a sudden on/off-set of the pulse in the leads, thus only giving an instantaneous reactance contribution in the energy current. As motivated in Ref. [47], the heat and energy transport can also be described as the transport from deep within the leads to get a good description in the case of a step-like bias pulse.

Using standard methods we can write the particle current as

$$I_\chi^N(t) = -\frac{2}{\hbar} \text{sp} \int_{-\infty}^t (\Sigma_\chi^>(t, t') \mathbf{G}^<(t', t) + \Sigma_\chi^<(t, t') \mathbf{G}^>(t', t)) dt', \quad (6)$$

where sp denotes the trace over spin-1/2 space. Using the generic separation of a matrix $\mathbf{A} = A_0 \sigma^0 + \boldsymbol{\sigma} \cdot \mathbf{A}_1$ in the fashion described in the previous section, we partition the current into a spin-independent and spin-dependent part according to $I_\chi^N(t) = I_{0\chi}^N(t) + I_{1\chi}^N(t)$, where

$$I_{0\chi}^N(t) = -\frac{4}{\hbar} \int_{-\infty}^t (\Sigma_{0\chi}^> G_0^< + \Sigma_{0\chi}^< G_0^>) dt', \quad (7a)$$

$$I_{1\chi}^N(t) = -\frac{4}{\hbar} \int_{-\infty}^t (\Sigma_{1\chi}^> \cdot \mathbf{G}_1^< + \Sigma_{1\chi}^< \cdot \mathbf{G}_1^>) dt'. \quad (7b)$$

Analogously, the spin-independent and spin-dependent part of the energy becomes

$$I_{0\chi}^E(t) = -\frac{4}{\hbar} \int_{-\infty}^t (\Sigma_{E0\chi}^> G_0^< + \Sigma_{E0\chi}^< G_0^>) dt', \quad (8a)$$

$$I_{1\chi}^E(t) = -\frac{4}{\hbar} \int_{-\infty}^t (\Sigma_{E1\chi}^> \cdot \mathbf{G}_1^< + \Sigma_{E1\chi}^< \cdot \mathbf{G}_1^>) dt'. \quad (8b)$$

Here, we defined the energy self-energy as $\Sigma_{E\chi\sigma}^{</>}(t, t') = \sum_{\mathbf{k} \in \chi} \varepsilon_{\mathbf{k}\sigma} |T_\chi|^2 g_{\mathbf{k}\sigma}(t, t')$ where we partition it in the same way as the regular self-energy as $\Sigma_E^{</>} = \Sigma_{E0}^{</>} \sigma^0 + \Sigma_{E1}^{</>} \cdot \boldsymbol{\sigma}$.

It is easy to distinguish the different contributions to the heat current using the decomposition as above. In the same manner we can define the heat current as $I_\chi^Q(t) = I_{0\chi}^Q(t) + I_{1\chi}^Q(t)$,

where we clearly see that $I_{0\chi}^Q(t)$ represents the heat current related to the Peltier effect, while $I_{1\chi}^Q(t)$ is the heat current related to the spin and spin-dependent Peltier effect.

We also note that in order to have a spin-driven heat current we need to have magnetic leads as the spin-dependent self-energies need to be finite. This can easily be seen by noting that the spin-dependence of the self-energies are governed by the lead GF and the tunneling coupling Γ^χ . This is also consistent with the fact that there needs to be a finite spin accumulation to get a spin Peltier effect.

D. Single-molecule spin dynamics

The local spin dynamics is calculated using our previously developed generalized spin-equation of motion (SEOM) [36], that is,

$$\dot{\mathbf{S}}(t) = \mathbf{S}(t) \times \left(-g\mu_B \mathbf{B}_0^{\text{eff}}(t) + \frac{1}{e} \int \mathbb{J}(t, t') \cdot \mathbf{S}(t') dt' \right). \quad (9)$$

Here, $\mathbf{B}_0^{\text{eff}}(t)$ is the effective magnetic field acting on the spin, defined by $g\mu_B \mathbf{B}_0^{\text{eff}}(t) = g\mu_B \mathbf{B}^{\text{ext}} + v\mathbf{m}(t) - \int \mathbf{j}(t, t') dt' / e$, where the second contribution is the local magnetic occupation, defined as $\mathbf{m}(t) = \langle \mathbf{s}(t) \rangle = \langle \psi(t)^\dagger \boldsymbol{\sigma} \psi(t) \rangle / 2 = \text{Im sp } \boldsymbol{\sigma} \mathbf{G}^<(t, t) / 2$, and the third term is the internal magnetic field due to the electron flow. The field $\mathbb{J}(t, t')$ is the dynamical exchange coupling between spins at different times.

We remark that despite the semi-classical nature of the generalized SEOM, it incorporates the underlying quantum nature of the junction through the dynamical fields \mathbf{j} and \mathbb{J} . This is specially important in the transient regime, since the classical Landau-Lifshitz-Gilbert equation provides an inadequate description of rapid changes [48].

The internal magnetic field due to the electron flow is defined as $\mathbf{j}(t, t') = iev\theta(t-t') \langle [s^{(0)}(t), \mathbf{s}(t')] \rangle$. The on-site energy distribution is represented by $s^{(0)} = \sum_\sigma \varepsilon_\sigma d_\sigma^\dagger d_\sigma$. The two-electron propagator is, here, approximated by decoupling into single electron nonequilibrium GF according to

$$\mathbf{j}(t, t') \approx iev\theta(t-t') \text{sp} \epsilon \left(\mathbf{G}^<(t', t) \boldsymbol{\sigma} \mathbf{G}^>(t, t') - \mathbf{G}^>(t', t) \boldsymbol{\sigma} \mathbf{G}^<(t, t') \right), \quad (10)$$

where $\epsilon = \text{diag}\{\varepsilon_\uparrow, \varepsilon_\downarrow\}$. This internal field mediates both the magnetic field generated by the charge flow as well as the effect of the external magnetic field causing the Zeeman split in the QD.

The spin susceptibility tensor $\mathbb{J}(t, t') = i2ev^2\theta(t-t') \langle [\mathbf{s}(t), \mathbf{s}(t')] \rangle$ mediates the interactions between the localized magnetic moment at the times t and t' . Decoupling into single electron GFs, we can write

$$\mathbb{J}(t, t') \approx \frac{ie}{2} v^2 \theta(t-t') \text{sp} \boldsymbol{\sigma} \left(\mathbf{G}^<(t', t) \boldsymbol{\sigma} \mathbf{G}^>(t, t') - \mathbf{G}^>(t', t) \boldsymbol{\sigma} \mathbf{G}^<(t, t') \right). \quad (11)$$

This current mediated interaction can be decomposed into an isotropic Heisenberg interaction, J_H , and the anisotropic

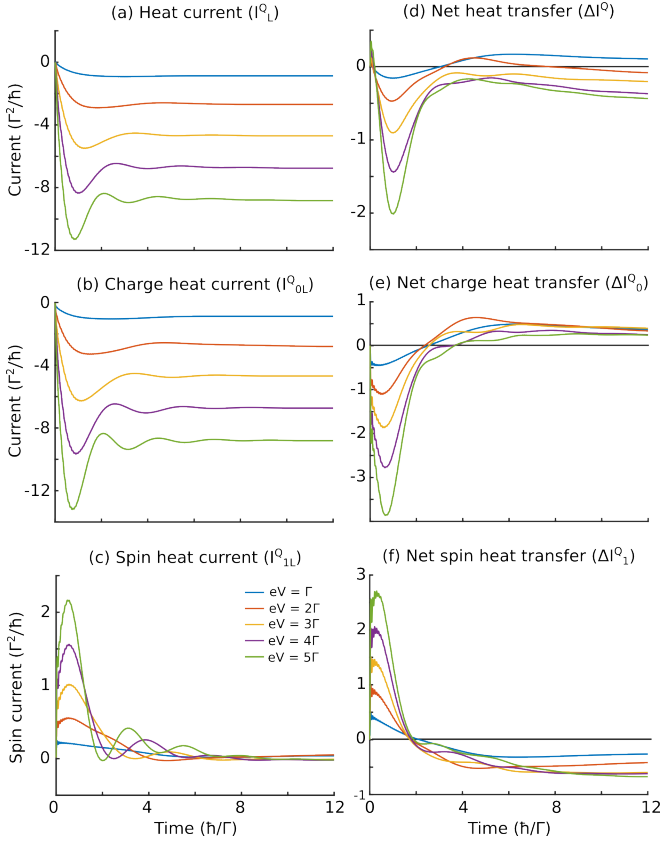


FIG. 2: The evolution of the heat currents and entropy production in the SMM due to the on-set of a bias voltage for different bias voltages V . First column indicates (a) the heat current flowing from the left lead I_L^Q , split into its (b) charge I_{0L}^Q and (c) spin I_{1L}^Q components. Second column indicates (a) the net heat transfer ΔI^Q split into its (b) charge ΔI_0^Q and (c) spin ΔI_1^Q components. Here, we used $t_0 = 0$, $\Gamma_0 = \Gamma$, $v = \Gamma/2$, $p_L = p_R = 0.5$, $T = 0.0862 \Gamma/k_B$ and $B = 0.1158 \Gamma/g\mu_B$.

Dzyaloshinski-Moriya (DM), \mathbf{D} , and Ising, \mathbb{I} , interactions [35, 36]. By doing the decomposition we can get an idea of the local anisotropies and energy landscape of the SMM.

III. RESULTS

We simulate the results for an applied time-dependent bias voltage initiating the dynamical evolution of the localized spin. At a time t_0 there is a sudden on-set of a bias voltage V that introduces a chemical potential $\mu_L = -\mu_R = eV\theta(t-t_0)/2$ to the leads. In order to have a finite spin-dependent heat current we use magnetic leads, i.e., a finite Γ_1^X , by setting $p_L = p_R = 0.5$. We also set the temperature of the leads to be the same in order to have pure Peltier contribution in the current and no Fourier heat transfer. We represent the quantities in terms of the model parameter Γ , which represent the tunneling coupling Γ_0 in all figures except Fig. 3 where the tunneling coupling is varied.

The heat current is simulated for different bias voltages, see

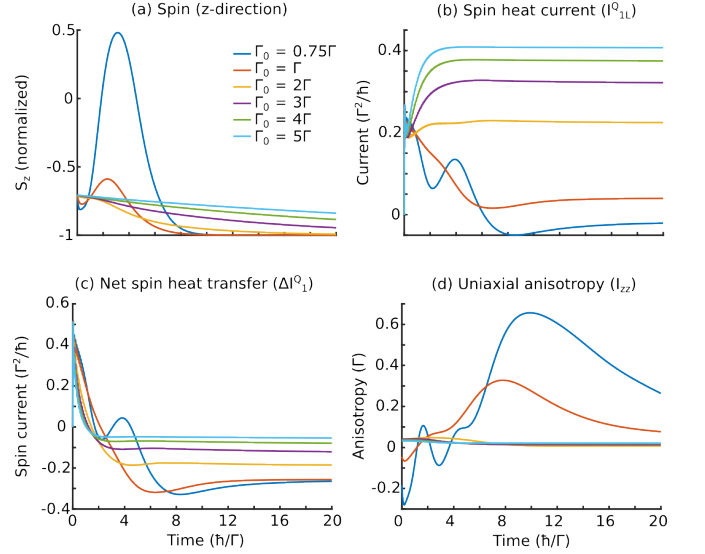


FIG. 3: The evolution of (a) the spin, (b) the spin-dependent heat current, (c) the spin-dependent net heat transfer and (d) uniaxial anisotropy for different tunneling coupling Γ_0 . Other parameters as in Fig. 2.

Fig. 2. Here, the first column indicates the heat flow from the left lead into the QD. The full heat current is shown in Fig. 2(a) and is then split into its (b) charge- and (c) spin-dependent components. As we can see, the majority of the contribution due to the charge heat flow is negative. The negative heat flow is due to the particle current directed from the left lead to the right, as seen in Eq. 5c. The spin-dependent heat current, shown in Fig. 2(c), is positive, thus counteracts the charge heat current. This contribution quickly vanishes for longer times and the main contribution to the heat flow is due to the charge flow in the system. It is although clear that a spin Peltier effect is of importance in the transient regime and will create a spin-dependent heat flow.

The second column of Fig. 2 shows the net heat transfer in the system. We define it as $\Delta I^Q = I_L^Q - I_R^Q$, thus, requiring the net contribution due to particle current to be zero in the steady state. It can easily be motivated as $I_L^Q - I_R^Q = I_L^E - \mu_L I_L^N - (I_R^E - \mu_R I_R^N) = I_L^E - I_R^E - \mu_L (I_L^N + I_R^N)$, where $I_L^N + I_R^N$ is zero in the steady-state regime because of particle conservation. As a result the long term behavior of the net heat transfer will be dominated by the energy current.

The net heat transfer constitutes the heat related change of entropy in the molecule. This gives an indication of the entropy change in the system. To get a full description of the entropy and to comply with the second law of thermodynamics the internal entropy production need to be considered to account for the transient dynamics [44]. There will also be additional terms related to the derivative of the driving force related to the system-bath coupling [40–43], but as we are considering a sudden onset this contribution can be considered to be negligible except for $t = t_0$. We also note that there is entropy related to the localized spin which is not treated in the current formalism.

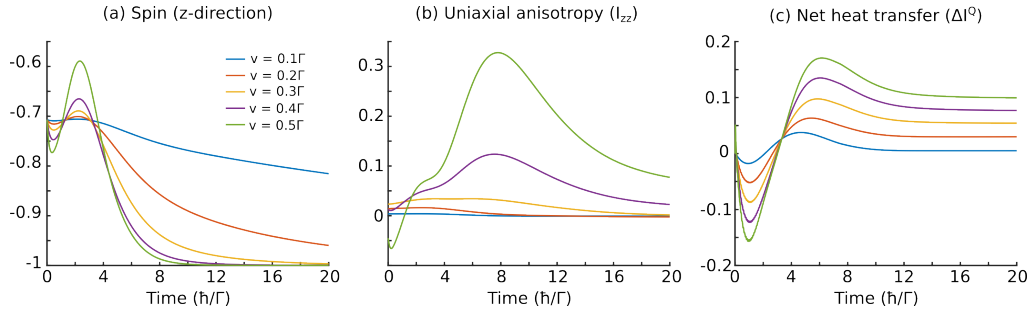


FIG. 4: The evolution of (a) the spin, (b) uniaxial anisotropy and (c) net heat transfer for different exchange coupling v . Other parameters as in Fig. 2.

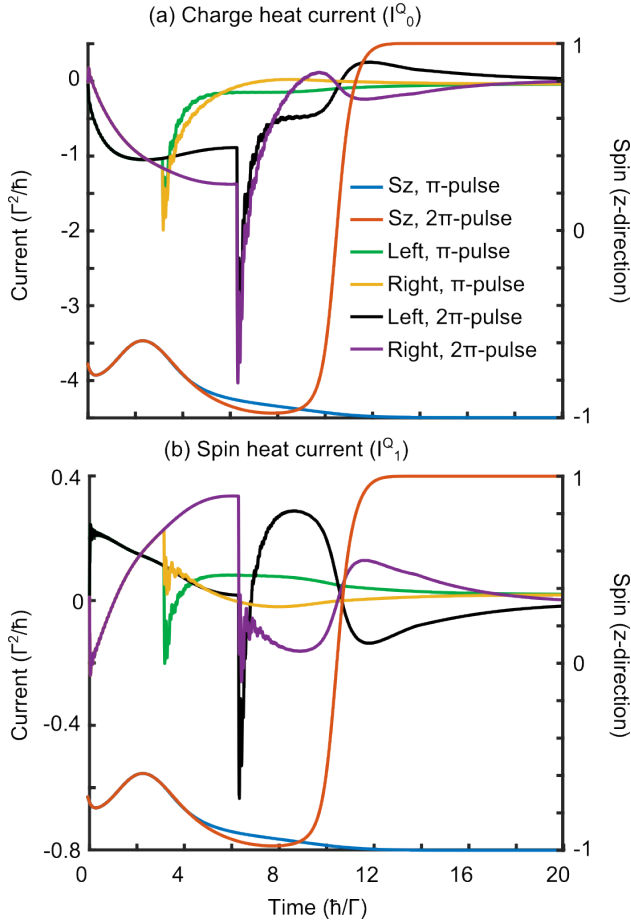


FIG. 5: The evolution of (a) charge-dependent heat current from the left and right lead (left axis) after a $eV(t_1 - t_0) = \pi$ and 2π -pulse resulting in a spin-flip of the localized magnetic moment (right axis) and heat currents to the left and right lead. (b) Spin-dependent heat flow from left and right lead due to π and 2π -pulses. Other parameters as in Fig. 2.

Fig. 2(d) shows the net heat transfer due to both (e) charge and (f) spin components. As can be seen in Fig. 2(e)-(f) is that the net heat transfer due to the charge flow is initially negative and then positive, and the opposite for the spin-dependent component. A negative contribution results in local heating of

the magnetic molecule, while a positive results in local cooling. It is because of that we have defined the heat current as heat flowing from the leads into the molecule. Increasing the bias voltage will change the strength of the different contributions and the magnitude of the spin-dependent net heat transfer production will increase, creating a net reversal in the heat transfer. Thus, it will change from continuously cooling the molecule to heat it up.

Next, we look at varying the tunneling coupling Γ_0 . This would relate to the coupling between a STM tip and a molecule, which both determines the damping of the system and the anisotropy of the molecule [32]. In Fig. 3 the results are shown for different couplings Γ_0 . Fig. 3(a) shows the resulting spin dynamics for the z-projection of the spin. As can be seen in the figure, the larger couplings damp the dynamics and reduces the oscillations of the spin. This can also be seen in the spin-dependent heat current in Fig. 3(b). Here, a higher coupling strength reach a steady state faster and gives an increase in the spin-dependent heat current. In the case of the spin-dependent net heat transfer, shown in Fig. 3(c), the increased tunneling coupling destroys the contribution and the spin-dependent net heat transfer goes to zero.

The damping behavior in the spin dynamics of the SMM and coupling dependent change of the spin-dependent heat current is an interplay between the tunneling coupling and the local exchange interaction within the SMM. Small tunneling couplings Γ_0 in comparison to the exchange coupling v will create a less damped system and larger anisotropies. In Fig. 3(d) the time-dependent evolution of the uniaxial anisotropy (I_{zz}) is shown for the different tunneling couplings. As seen, the local anisotropies vary greatly for small tunneling coupling. In the case of larger couplings, the uniaxial anisotropies almost vanish. Thus, there is a large change of the local spin environment due to the tunneling coupling, creating a significant change in the spin-dependent heat characteristics as seen in Fig. 3(b)-(c).

Varying the exchange coupling v controls the effect of the local magnetic moment on the surrounding electronic structure in the molecule as well as the dynamics of the magnetic moment. We see in Fig. 4(a) that starting with a finite exchange coupling v initiates the dynamics of the local magnetic moment and then leads to faster dynamics for an increasing v . In the same way as for decreasing tunneling coupling, there will be an effect on the local anisotropies of the molecule due

to increasing exchange coupling, see Fig. 4(b) (cf. Fig. 3(d)). The net heat transfer is zero for zero exchange coupling and then increases as the exchange coupling increases, see Fig. 4(c).

As we have seen in the results, the net heat transfer is finite in the junction for small tunneling couplings Γ_0 and a finite exchange v . For increasing bias it will become negative due to the spin-dependent net heat transfer, thus heating up the molecule. In order to achieve a net heat transfer we need to have magnetic leads and a finite exchange. Thus, one can connect the cooling/heating of the molecule to the spin dynamics and the interaction between the spin-dependent electron channels and the localized spin.

We now turn to consider the effect of pulses in the heat currents in the system. We do this by applying a finite pulse that start at t_0 and end at t_1 . Due to the phase-dependence in the integration kernel in the self-energy in Eq. 4, a $eV(t_1 - t_0) = 2\pi$ -pulse will create a switching of the spin as shown in Ref. [49]. Thus, we apply both a π - and a 2π -pulse in order to simulate two different spin regimes and see the effect in the heat current related to the switching. In Fig. 5(a) we show the results for the charge-dependent heat current. We see clearly the switching behavior due to the 2π -pulse. In the case of the heat current there is a sudden change when the pulse is shut of due to the recombination of energy in the system, i.e., related to the energy current. In Fig. 5(b) the spin-dependent heat current is shown with a similar behavior as the charge-dependent heat transfer. Interestingly, in the case of a π -pulse, the heat current will oscillate around zero and there is no significant net heat transfer. In the case of 2π -pulse there is an asymmetric behavior, creating a net heat transfer right before the switching of the spin. After the switching has taken place both the

charge- and spin-dependent heat current oscillate about zero giving no net heat transfer. Thus, there is a clear signature in the heat current and net heat transfer related to the switching of the localized magnetic moment of the SMM. This could be both of interest for probing switching in a SMM as well as to enhance the thermoelectric efficiency of SMM devices.

IV. CONCLUSIONS

We have investigated spin-dependent heat signatures in a SMM and its connection to the SMM spin dynamics. We have shown that signatures in the heat current can be attributed to both charge and spin degrees of freedom. The latter can be related to the spin-dependent and spin Peltier effect. Distinct features in the heat flow can be connected to the spin-dependent drive and fluctuations which opens possibilities to engineer thermoelectric devices using driven SMMs. Increasing the bias voltage can introduce a reversal of the net heat transfer. By tuning the tunneling coupling or the exchange coupling, the local anisotropies of the SMM can be modulated, which can lead to a significant decrease of the spin-dependent net heat transfer in the system. Finally, we point out a correlation between modulations in the heat flow and switching of the spin.

V. ACKNOWLEDGMENTS

The authors thank A. Sisman, P. Oppeneer and R. López for fruitful discussions. The work is supported by Vetenskaprådet, SNIC 2018/8-29 and Colciencias (The Colombian Department for Science, Technology and Innovation).

-
- [1] Y. Dubi and M. Di Ventra, *Rev. Mod. Phys.* **83**, 131 (2011).
 [2] J. Xiao, G. E. W. Bauer, K. C. Uchida, E. Saitoh, and S. Maekawa, *Phys. Rev. B* **81**, 214418 (2010).
 [3] K. Uchida, J. Xiao, H. Adachi, J. Ohe, S. Takahashi, J. Ieda, T. Ota, Y. Kajiwara, H. Umezawa, H. Kawai, et al., *Nat Mater* **9**, 894 (2010).
 [4] S. T. Goennenwein and G. E. Bauer, *Nat Nano* **7**, 145 (2012).
 [5] G. E. Bauer, E. Saitoh, and B. J. Van Wees, *Nat Mater* **11**, 391 (2012).
 [6] H. Adachi, K.-i. Uchida, E. Saitoh, and S. Maekawa, *Rep. Prog. Phys.* **76**, 036501 (2013).
 [7] R.-Q. Wang, L. Sheng, R. Shen, B. Wang, and D. Y. Xing, *Phys. Rev. Lett.* **105**, 057202 (2010).
 [8] M. Misiorny and J. Barnaś, *Phys. Rev. B* **89**, 235438 (2014).
 [9] M. Misiorny and J. Barnaś, *Phys. Rev. B* **91**, 155426 (2015).
 [10] J. W. Sharples, D. Collison, E. J. L. McInnes, E. Palacios, and M. Evangelisti, *Nat Commun* **5**, 6321 (2014).
 [11] Y. Wang, N. S. Rogado, R. J. Cava, and N. P. Ong, *Nature* **423**, 425 (2003).
 [12] Y. Dubi and M. Di Ventra, *Phys. Rev. B* **79**, 081302 (2009).
 [13] R. Świrkowicz, M. Wierzbicki, and J. Barnaś, *Phys. Rev. B* **80**, 195409 (2009).
 [14] P. Trocha and J. Barnaś, *Phys. Rev. B* **85**, 085408 (2012).
 [15] I. Weymann and J. Barnaś, *Phys. Rev. B* **88**, 085313 (2013).
 [16] J. Ren, J. Fransson, and J.-X. Zhu, *Phys. Rev. B* **89**, 214407 (2014).
 [17] Ł. Karwacki, P. Trocha, and J. Barnaś, *J. Phys.: Condens. Matter* **25**, 505305 (2013).
 [18] I. Weymann, *Scientific Reports* **6**, 19236 (2016).
 [19] Ł. Karwacki and P. Trocha, *Phys. Rev. B* **94**, 085418 (2016).
 [20] S.-Y. Hwang, R. López, and D. Sánchez, *Phys. Rev. B* **94**, 054506 (2016).
 [21] J. P. Ramos-Andrade, F. J. Peña, A. González, O. Ávalos-Ovando, and P. A. Orellana, *Phys. Rev. B* **96**, 165413 (2017).
 [22] P. Trocha and J. Barnaś, *Phys. Rev. B* **95**, 165439 (2017).
 [23] A. Crépieux, F. Āimkovic, B. Cambon, and F. Michelini, *Phys. Rev. B* **83**, 153417 (2011).
 [24] M. B. Tagani and H. R. Soleimani, *Int. J. Thermophysics* **35**, pp. 136–144 (2012).
 [25] W. Liu, K. Sasaoko, T. Yamamoto, T. Tada, and S. Watanabe, *Jap. J. Appl. Phys.* **51**, 094303 (2012).
 [26] H. Zhou, J. Thingna, P. Hånggi, J.-S. Wang, and B. Li, *Scientific reports* **5**, 14870 (2015).
 [27] A.-M. Daré and P. Lombardo, *Phys. Rev. B* **93**, 035303 (2016).
 [28] S. Loth, K. von Bergmann, M. Ternes, A. F. Otte, C. P. Lutz, and A. J. Heinrich, *Nat Phys* **6**, 340 (2010).
 [29] A. A. Khajetoorians, J. Wiebe, B. Chilian, and R. Wiesendanger, *Science* **332**, 1062 (2011).
 [30] A. A. Khajetoorians, B. Baxevanis, C. Hübner, T. Schlenk, S. Krause, T. O. Wehling, S. Lounis, A. Lichtenstein,

- D. Pfannkuche, J. Wiebe, et al., *Science* **339**, 6115 (2013).
- [31] S. Fahrenndorf, N. Atodiresei, C. Besson, V. Caciuc, F. Matthes, S. Blügel, P. Kögerler, D. E. Bürgler, and C. M. Schneider, *Nat Commun* **4**, 3425 (2013).
- [32] B. W. Heinrich, L. Braun, J. I. Pascual, and K. J. Franke, *Nano Lett.* **15**, 4024 (2015).
- [33] V. E. Campbell, M. Tonelli, I. Cimatti, J.-B. Moussy, L. Tortech, Y. J. Dappe, E. Rivière, R. Guillot, S. Delprat, R. Mattana, et al., *Nat Commun* **7**, 13646 (2016).
- [34] F. D. Natterer, K. Yang, W. Paul, P. Willke, T. Choi, T. Greber, A. J. Heinrich, and C. P. Lutz, *Nature* **543**, 226 (2017).
- [35] J. Fransson, J. Ren, and J.-X. Zhu, *Phys. Rev. Lett.* **113**, 257201 (2014).
- [36] H. Hammar and J. Fransson, *Phys. Rev. B* **94**, 054311 (2016).
- [37] T. Saygun, J. Bylin, H. Hammar, and J. Fransson, *Nano Lett.* **16**, 2824 (2016).
- [38] J. D. V. Jaramillo and J. Fransson, *J. Phys. Chem. C* **121**, 27357 (2017).
- [39] J. D. Vasquez Jaramillo, H. Hammar, and J. Fransson, *ACS Omega* **3**, 6546 (2018).
- [40] M. F. Ludovico, J. S. Lim, M. Moskalets, L. Arrachea, and D. Sánchez, *Phys. Rev. B* **89**, 161306 (2014).
- [41] M. F. Ludovico, M. Moskalets, D. Sánchez, L. Arrachea, D. Sanchez, and L. Arrachea, *Phys. Rev. B* **94**, 035436 (2016).
- [42] A. Bruch, M. Thomas, S. Viola Kusminskiy, F. Von Oppen, and A. Nitzan, *Phys. Rev. B* **93**, 115318 (2016).
- [43] P. Haughian, M. Esposito, and T. L. Schmidt, *Phys. Rev. B* **97**, 085435 (2018).
- [44] M. Esposito, M. A. Ochoa, and M. Galperin, *Phys. Rev. Lett.* **114**, 080602 (2015).
- [45] M. Esposito, M. A. Ochoa, and M. Galperin, *Phys. Rev. B* **92**, 235440 (2015).
- [46] Y. Dubi and M. Di Ventra, *Nano Letters* **9**, 97 (2009).
- [47] L. Liu, O. J. Lee, T. J. Gudmundsen, D. C. Ralph, and R. A. Buhrman, *Phys. Rev. Lett.* **109**, 096602 (2012).
- [48] H. Hammar and J. Fransson, *Phys. Rev. B* **96**, 214401 (2017).
- [49] H. Hammar and J. Fransson, arXiv:1806.07092 (2018).